Author(s): Nauha, Elisa; Kolehmainen, Erkki; Nissinen, Maija

Title: Packing incentives and a reliable N–H...N–pyridine synthon in co-crystallization of bipyridines with two agrochemical actives

Year: 2011

Version:

Please cite the original version:

Nauha, E., Kolehmainen, E., & Nissinen, M. (2011). Packing incentives and a reliable N–H...N–pyridine synthon in co-crystallization of bipyridines with two agrochemical actives. CrystEngComm, 13(21), 6531-6537. https://doi.org/10.1039/C1CE05730H

CrystEngComm

Dynamic Article Links ►

Cite this: DOI: 10.1039/c0xx00000x

www.rsc.org/crystengcomm

ARTICLE TYPE

Packing incentives and a reliable N-H•••N-pyridine synthon in co-crystallization of bipyridines with two agrochemical actives

Elisa Nauha, Erkki Kolehmainen and Maija Nissinen*

Received (in XXX, XXX) Xth XXXXXXXXX 20XX, Accepted Xth XXXXXXXXX 20XX

DOI: 10.1039/b000000x

The co-crystallization of agrochemical actives thiophanate-methyl and thiophanate-ethyl with 2,2'-bipyridine, 4,4'-bipyridine and 1,2-bis(4-pyridyl)ethane was investigated with conventional crystallization, the slurry method and liquid-assisted grinding. Co-crystals of both thiophanates with all bipyridines were found and the structures solved with single crystal X-ray diffraction. Whereas the 2,2'-bipyridine co-crystals seem to form because of a combination of weak interactions, and in the case of the thiophanate-methyl, partly because of close packing incentives, the 4,4'-bipyridine and 1,2-bis(4-pyridyl)ethane co-crystals form mainly because of a favourable N-H•••N-pyridine hydrogen bonding synthon.

Introduction

The phenomenon of co-crystallization[1,2] is important for pharmaceutical[3-5], agrochemical[6,7] and other industrial applications because of the different and sometimes improved properties of co-crystals of active ingredients compared to those of the parent molecules. For pharmaceutical applications the goal of co-crystal forms is usually to increase the solubility and bioavailability of the active ingredient while maintaining the physical stability of the dosage form, but for agrochemical actives, which are often administered as slurry formulations in water, the goal is to lower the solubility of the active to make a more stable formulation and stop the active being washed away too soon once administered.

In a simplified model co-crystallization can be seen to arise for two different reasons, either close packing or favorable hydrogen bonding interactions[1,8]. The strategy to find co-crystals that form because of close packing requires a trial and error approach since it is very hard to predict, if a pair of molecules can pack tightly. For co-crystals caused by favorable hydrogen bonding interactions one can make educated guesses about possible co-crystal formers based on knowledge about hydrogen bonding synthons[9] with, for example, the help of the CCDC database. In practice, however, packing in crystals is influenced by an intricate combination of close packing incentives, hydrogen bonding and other interactions and therefore there is as yet no reliable way to design co-crystals.

Previously, we have been investigating the polymorphism and versatile solvate formation of two agrochemical actives, thiophanate-methyl (TM)[10] and thiophanate-ethyl (TE)[11] (Scheme 1), and decided now to examine co-crystallization with common co-crystal formers, namely 4,4'-bipyridine (44bp)[12-17] and 2,2'-bipyridine (22bp)[18] (Scheme 1) as pyridine solvates of TM and TE are also known. Due to the success with the first bipyridines, crystallizations with the similar 1,2-bis(4-pyridyl)ethane (44bpe) (Scheme 1) were also attempted. An important goal was to see how much the difference of one carbon at the end of the chains in TE, in comparison to TM, affects the crystallization behavior and packing of the molecules.

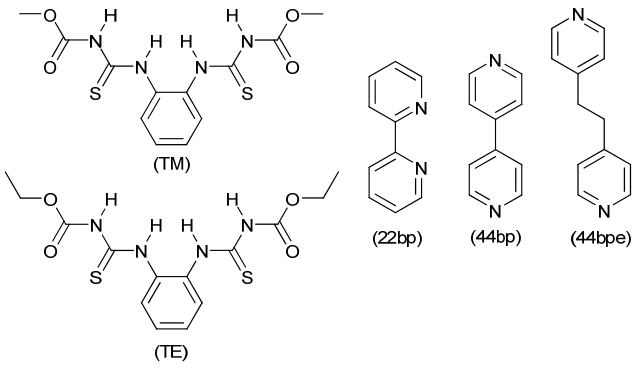

Scheme 1 Molecular structures of thiophanate-methyl (TM), thiophanate-ethyl (TE), 2,2'-bipyridine (22bp) and 4,4'-bipyridine (44bp), 1,2-bis(4-pyridyl)ethane (44bpe)

Experimental

Materials

TM (IUPAC: dimethyl 4,4'-(*o*-phenylene)bis(3-thioallophanate)) of 99.8% purity from BASF, TE (IUPAC: diethyl 4,4'-(*o*-phenylene)bis(3-thioallophanate)) of 99% purity from Chem Service, 2,2'-bipyridine from Merck, 4,4'-bipyridine from Sigma-Aldrich, 1,2-bis(4-pyridyl)ethane (99%) from Aldrich, distilled water and solvents of analytical purity (min 99%) were used in the crystallization, slurry and milling experiments.

Slurries

Slurries of TM with the 22bp and 44bp were carried out in a

acetonitrile:water solution. The slurries were mixed for three days at 50°C, filtered with suction and let dry in open vessels.

Table 1 Crystal data and collection parameters for the co-crystal structures

Compound reference	TM-22bp	TE-22bp	TM-44bp	TE-44bp	TM-44bpe	TE-44bpe
Chemical formula	$2(C_{12}H_{14}N_4O_4S_2)$ $\bullet 1.5(C_{10}H_8N_2)$ $\bullet C_2H_3N$	$C_{14}H_{18}N_4O_4S_2$ $\bullet 0.5(C_{10}H_8N_2)$	$C_{12}H_{14}N_4O_4S_2$ $\bullet 0.5(C_{10}H_8N_2)$	$C_{14}H_{18}N_4O_4S_2$ $\bullet C_{10}H_8N_2$	$2(C_{12}H_{14}N_4O_4S_2)$ $\bullet C_{12}H_{12}N_2$	$2(C_{14}H_{18}N_4O_4S_2)$ $\bullet C_{12}H_{12}N_2$
Formula Mass	960.11	448.54	420.48	526.63	869.02	925.12
Crystal system	Triclinic	Monoclinic	Triclinic	Triclinic	Triclinic	Triclinic
a/Å	10.6193(3)	8.3860(7)	9.0382(2)	11.8193(4)	9.0972(2)	11.9780(10)
b/Å	15.0562(4)	17.2950(12)	9.5723(2)	12.8098(5)	9.5762(2)	14.1211(12)
c/Å	16.2601(4)	15.4566(11)	12.5370(3)	26.3527(10)	23.8891(3)	14.9536(12)
α/°	108.694(4)	90.00	100.183(3)	91.574(2)	86.224(1)	107.572(4)
β/°	95.323(3)	98.93(3)	104.203(3)	95.655(2)	88.273(1)	106.503(5)
γ/°	109.312(4)	90.00	101.444(3)	100.640(3)	88.214(1)	91.062(4)
Unit cell volume/Å^3	2265.87(10)	2214.6(3)	1001.16(4)	3897.9(2)	2074.79(7)	2296.8(3)
Space group	*P*-1	*P*2(1)/*c*	*P*-1	*P*-1	*P*-1	*P*-1
Z	2	4	2	6	2	2
Meas. reflns.	10805	6504	4322	18442	10604	9982
Indep. reflns.	7733	3778	3298	13511	7144	7030
R_{int}	0.0585	0.0975	0.1194	0.1463	0.1069	0.1410
Final R_1 values ($I > 2\sigma(I)$)	0.0517	0.0713	0.0657	0.0802	0.0604	0.0688
Final $wR(F^2)$ values ($I > 2\sigma(I)$)	0.1257	0.1812	0.1788	0.2103	0.1459	0.1382
Final R_1 values (all data)	0.0722	0.1077	0.0735	0.1094	0.0832	0.1494
Final $wR(F^2)$ values (all data)	0.1394	0.2117	0.1882	0.2389	0.1628	0.1758
Goodness of fit on F^2	1.032	1.039	1.069	1.071	1.043	1.018

Crystallizations

Equimolar (1:1) amounts (< 40 mg in total) of the compounds were weighed and dissolved in acetonitrile, the solutions were transferred to clean crystallization test tubes, the test tubes covered with parafilm with a few holes and the solvent was let evaporate in room temperature. Crystallization of TM with 22bp and TE with 44bp was also attempted in ethanol with and without seeding by the grinded samples, but the crystallizations produced single crystals of the ethanol solvate of TM[10] and form I of TE[11], respectively.

Grinding

Liquid-assisted grinding was carried out on a Retsch MM 200 ball mill in 10 ml milling vessels for 20 min with an oscillation frequency of 20 s^{-1}. 50 mg of TM/TE and a molar amount of 22bp or 44bp, according to the ratio in the co-crystal structures, were weighed and a few drops of 1:1 water:ethanol solution were added to the milling vessels. All but the TE – 44bp mixture produced PXRD patterns similar to the calculated patterns from the structures. For the TE - 44bp mixture and the TM - 22bp mixture, milling was also done with 3 drops of 25% MeCN in water to confirm the results.

Thermomicroscopy

The behavior of the 22bp and 44bp co-crystals during heating was studied under polarized light with a Mettler FP82HT hot stage connected to a Mettler FP90 central processor with an Olympus BH-2 microscope. The primary heating rate used was 10°C/min from 30°C to melting/decomposition of the sample.

PXRD

For powder X-ray diffraction analyses the samples were pressed to a zero background silicon plate sample holder and measured on a PANalytical X'Pert Pro system in reflection mode with non-monochromated Cu-radiation. A 2θ-angle range of 5–35° and a step time of 38 s were used with step resolution of 0.0167°. Figures were drawn with X'Pert HighScore Plus[19].

Single crystal X-ray diffraction

The X-ray diffraction data were collected on a Nonius Kappa CCD diffractometer with an Apex II detector, using graphite-monochromated CuKα radiation (λ = 1.54178 Å) at 173 K. The structures were solved by direct methods, refined, and expanded by Fourier techniques with the SHELX-97 software package[20]. Absorption correction was performed with Denzo 1997[21]. All non-hydrogen atoms were refined anisotropically. Hydrogen atoms were placed in idealized positions, or in the case of hydrogen bonding hydrogens, found from the electron density map and included in structure factor calculations. The N-H hydrogen atoms found in the electron density map were restrained to a distance of 0.91 Å to give the best fit to the X-ray data and to ensure stable refinement. Pictures of the structures were drawn with Mercury[22]. Crystal data and collection parameters of the structures are presented in Table 1.

^{13}C CP/MAS NMR

The ^{13}C CP/MAS NMR spectra were measured of the slurried TM samples with a Bruker Avance 400 FT NMR spectrometer with a dual 4 mm CP/MAS probehead. The sample was packed in a 4 mm diameter ZrO_2 rotor, which was spun at 10 kHz rate at 296 or 373 K. Contact time for CP was 4 ms, pulse interval 4 s, time domain 2 K, which was zero filled to 8 K in frequency domain. Exponential window function with 5 Hz line broadening was used. 20 000 scans were acquired. ^{13}C shifts are referenced to the CO-signal of glycine (176.03 ppm) measured before the TM sample.

Results and discussion

The formation of the TM co-crystals with 4,4'-bipyridine and 2,2'-bipyridine was first observed in slurry experiments, with the

results confirmed by PXRD and ^{13}C CP/MAS NMR, after which they were also found to crystallize from solution. Co-crystals for TE were acquired directly with solution crystallization and used also in the liquid-assisted grinding and thermomicroscopy experiments. The 1,2-bis(4-pyridyl)ethane co-crystals were later acquired by solution crystallization for structural comparison.

^{13}C CP/MAS NMR results

High resolution solid state NMR and especially ^{13}C CP/MAS is nowadays often used as an aid or complementary technique in polymorph, solvate and co-crystal characterization.[10,23] In this work ^{13}C CP/MAS spectra were measured for the TM-22bp and TM-44bp co-crystals, acquired by the slurry method, as well as for pure TM alone (Fig. 1). The assignment of the spectra are based on the comparison with liquid state NMR spectra.

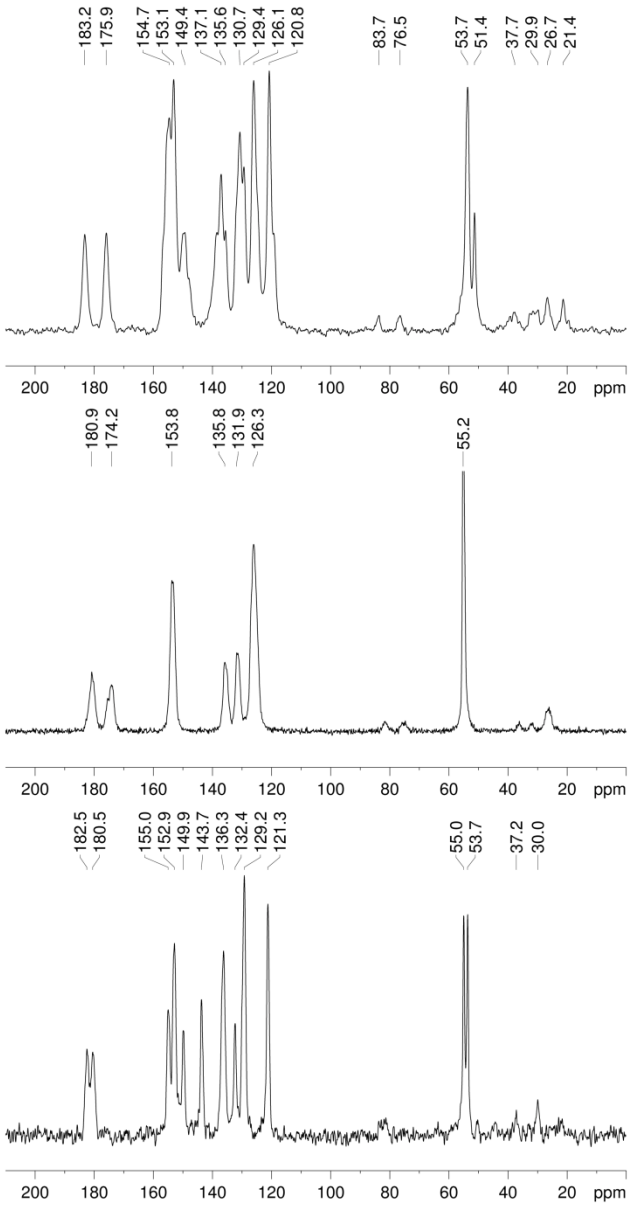

Fig. 1 CPMAS NMR of the TM-22bp co-crystal (top), TM form I (middle) and the TM-44bp co-crystal (bottom).

In the TM spectrum its C=O resonance is at 153.8 ppm and the aromatic carbons give three resonances as expected by symmetry reasons at 135.8, 131.9 and 126.3 ppm, respectively. C=S resonances are at 180.9 and 174.2 ppm, respectively. The tentative assignments of 2,2'-bipyridine resonances in the TM-22bp co-crystal spectrum are at 154.7 ppm (carbons 1,1'), at 149.4 (carbons 3,3'), at 137.1 ppm (carbons 5,5'), at 126.1 ppm (carbons 4,4') and at 120.8 ppm (carbons 6,6'), respectively. In the spectrum of TM-44bp, 4,4'-bipyridine signals are easy to find and assign at 149.9 ppm (carbons 3,3', 5,5'), at 143.7 ppm (carbons 1,1') and at 121.3 ppm (carbons 2,2', 6,6'). Differing from the TM sample in this co-crystal TM's CH_3O-signals exist as a doublet at 55.0 and 53.7 ppm. In TM-22bp spectrum CH_3O-group show two resonances but differing from TM-44bp with nonequal intensities.

Comparison of TM-44bp and TM-22bp spectra reveal that the chemical shift differences of C=S resonances (at 182.5 and 180.5 ppm) in TM-44bp co-crystal are clearly smaller than in TM-22bp where those are at 183.3 and 175.9 ppm, respectively. Taking into account the X-ray data (see below) it is quite clear to assign the TM-22bp resonance at 175.9 ppm to that one involved in hydrogen bonding. According to X-ray data C=S groups do not form hydrogen bonds in TM-44bp co-crystal, which explains the small shift difference. In pure TM sample the C=S shift difference is very close to that of TM-22bp suggesting similar hydrogen bonding behavior.

Surprisingly no trace from MeCN is visible in TM-22bp spectrum although the powder X-ray pattern of the sample is similar to the calculad pattern of a structure that contains also MeCN. This, together with the ability of the co-crystal to form also in ethanol solution, suggests that the co-crystal is still intact even without the MeCN.

Co-crystal structures with 2,2'-bipyridine

The MeCN solvate of the TM co-crystal with 2,2'-bipyridine crystallized in space group P-1 with a TM:22bp:MeCN ratio of 4:3:2, containing half of this in the asymmetric unit. The TM molecules build up double chains composed of rings of four TM molecules hydrogen bonded to each other (Fig. 2a). The rings are made with two hydrogen bonding arrangements, one of which is a R2,2(8) motif[24] composed of two N-H•••S hydrogen bonds and the other a second order R2,2(8) motif with one N-H•••S and one N-H•••O-C hydrogen bond. There is also a very weak C-H•••O-C bond supporting the connection with this motif. The rings of TM arrange into chains with a R2,2(12) motif of two N-H•••O=C hydrogen bonds.

One of the 22bp molecules resides right inside the ring of TM molecules while the other 22bp molecule along with the MeCN molecules is located between the TM double chains. There are edge-to-face aromatic interactions between the benzene rings of the TM molecules and the 22bp that are located outside the rings with ring centroid-C distances of 3.71 and 3.94 Å, and subsequent ring centroid-H distances of 2.78 and 3.03 Å.

The TE co-crystal with 2,2'-bipyridine crystallized in space group $P2_1/c$ with a molecule of TE and half a molecule of 22bp in the asymmetric unit, giving the ratio of 2:1. The TE molecules build up hydrogen bonded chains (Fig. 2b) with a R2,2(8) motif consisting of two N-H•••S hydrogen bonds. There are additionally only intramolecular N-H•••O=C hydrogen bonds in an S(6) motif. The chains of TM pack parallel to each other with

π-π stacking interactions to neighboring chains with ring distances of approximately 3.4 Å. The 22bp molecules are located in between the arms of the TE molecules in channels running through the structure in the direction of the crystallographic a-axis (Fig. 2b). There are weak hydrogen bonds between the 22bp nitrogens and the ethyl hydrogens of TE molecules in neighboring chains. The arrangement of TE molecules in the structure of this co-crystal is interestingly the same as that in the previously obtained isomorphous acetone, DCM, chloroform and dioxane solvates of TE[11] with the 22bp taking up the space of two solvent molecules.

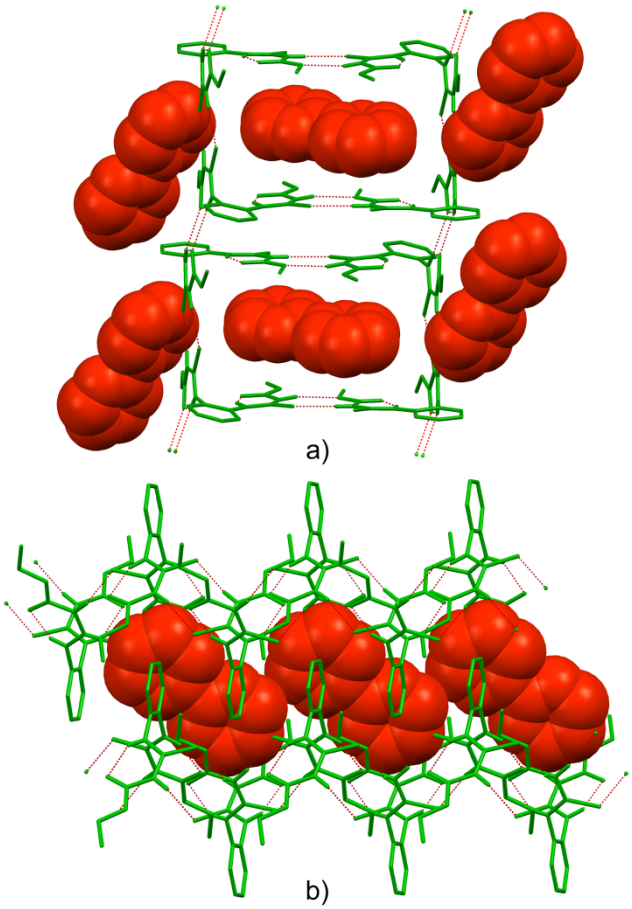

Fig. 2 (a) Rings of TM with 22bp in the MeCN solvate of the TM co-crystal with 22bp and (b) the channels of 22bp in the TE co-crystal with 22bp. MeCN molecules and C-H hydrogen atoms removed for clarity.

Co-crystal structures with 4,4'-bipyridine

In the TM•4,4'-bipyridine co-crystal the TM to 44bp ratio is 2:1, while in the TE 4,4'-bipyridine co-crystal the TE to 44bp ratio is 1:1. However, there are similarities in the hydrogen bonding patterns of these co-crystals (Fig. 3a and b). The similar hydrogen bonded unit consist of two molecules of TM/TE connected with a R2,2(12) motif of two N-H•••O=C hydrogen bonds, and two molecules of 44bp which are hydrogen bonded to this pair. The difference of the structures lies in the hydrogen bonding of these units into chains.

The TM co-crystal with 4,4'-bipyridine crystallized in space group P-1 with one molecule of TM and half a molecule of 44bp in the asymmetric unit. The R2,2(12) hydrogen bonded pairs are connected with hydrogen bonds to the 44bp molecules making up infinite parallel chains where a pair of TM molecules and a 44bp molecule alternate (Fig. 3a). Interestingly, in this structure the sulfurs are not involved in hydrogen bonding and one N-H hydrogen is also left without a hydrogen bond acceptor.

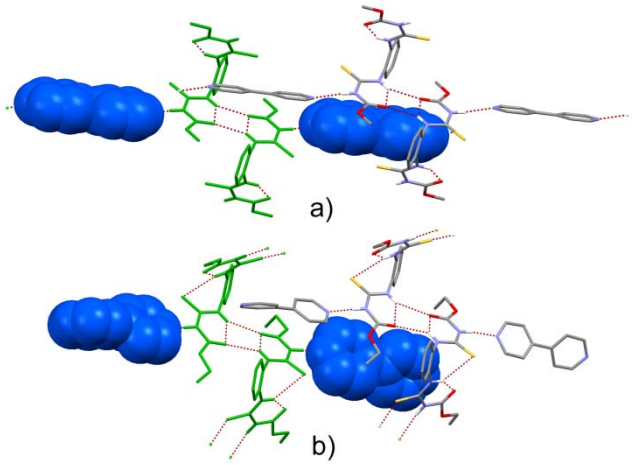

Fig. 3 Hydrogen bonding and packing in the (a) TM and (b) TE-44bp co-crystals with C-H hydrogen atoms removed for clarity.

The TE co-crystal with 4,4'-bipyridine crystallized in the space group P-1 with three molecules of TE and three molecules of 44bp in the asymmetric unit. The symmetrically different molecules of TE are fairly similar in conformation, with differences mostly in the orientation of the ethyl groups at the ends of the arms. The torsion angles of the ethyl group from the C=O groups are 170.2°, -156.1°, 165.1°, 179.2°, -88.9° and 155.1°. The symmetrically different molecules also have the same hydrogen bonds to neighboring molecules. The reason for so many molecules in the asymmetric unit seems to be the combined influence of the flexibility of conformation of the ends of the arms of the TE molecules and in the variable conformations of the 44bp molecules. The torsion angles between the rings of the 44bp molecules are 41.3°, 43.4° and 44.9°.

The R2,2(12) hydrogen bonded pairs are connected with a R2,2(8) motif of two N-H•••S hydrogen bonds to neighboring pairs forming hydrogen bonded chains of TE molecules in the structure (vertical direction in Fig. 3b). These chains pack parallel to each other with the 44bp molecules of the neighboring chains located partly in between the arms of the TE molecules. Unlike in the TM co-crystal, the other pyridine acceptor in the 44bp does not take part in hydrogen bonding.

Co-crystal structures 1,2-bis(4-pyridyl)ethane

Both the 1,2-bis(4-pyridyl)ethane co-crystals crystallized in spacegroup P-1 with a ratio of 2:1 (TM/TE:44bpe). Also in these co-crystals the TM/TE molecules make pairs connected with a R2,2(12) motif of two N-H•••O=C hydrogen bonds, and two molecules of 44bpe are hydrogen bonded to this pair.

In the The TM co-crystal with 1,2-bis(4-pyridyl)ethane there are two unconnected domains in the structure consisting of the symmetry unequivalent TM molecules and half molecules of 44bpe on an inversion center. In one case the pairs are only connected with hydrogen bonds to the bipyridine, similarly to the TM co-crystal with 44bp, making up chains, but in the other case

the hydrogen bonded pairs are connected with a D(2) N-H•••S motif to other TE molecules to build up double chains which then connect into sheets via the bipyridine molecules (Fig. 4a). The two domains make up sheets that stack up on each other in the crystal.

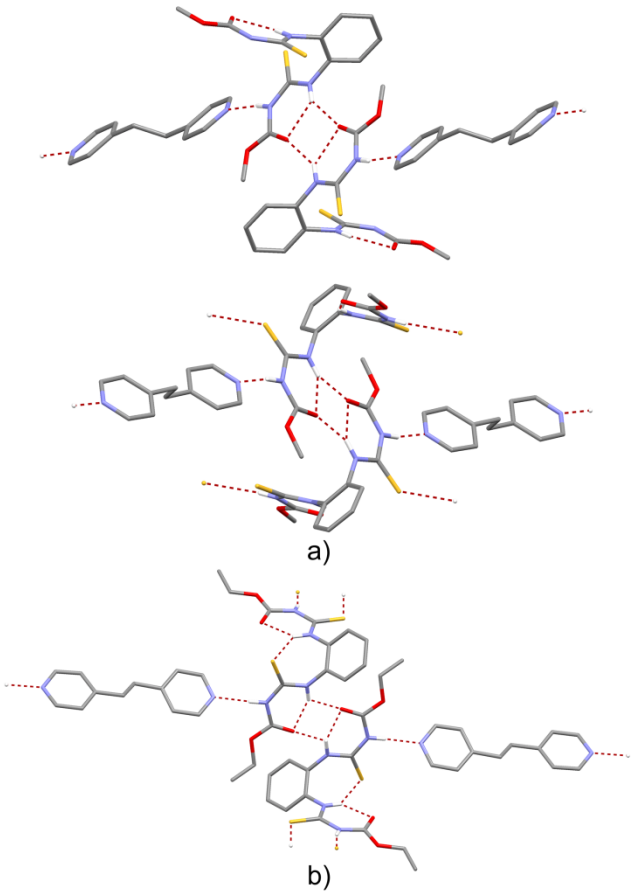

Fig. 4 Hydrogen bonded pairs in (a) the two domains of the TM bis(4-pyridyl)ethane co-crystals and (b) the TE 1,2-bis(4-pyridyl)ethane co-crystals with C-H hydrogen atoms removed for clarity.

In the TE co-crystal with 1,2-bis(4-pyridyl)ethane the hydrogen bonding in the between the TE molecules is identical to that in the TE co-crystal with 44bp, but additionally the TE chains are connected via the 44bpe molecules like in the TM co-crystal with 44bp (Fig. 4b). In the chains of TE pairs of the two symmetry unequivalent TE molecules connected with the R2,2(12) motif alternate.

Packing incentives

The packing coefficients[25] (Fig. 5) for co-crystal structures were calculated using the formula C(k) = Z*V(mol)/V(cell), where Z is the number of molecules in the unit cell, V(mol) is the molecular volume of the molecules[26], and V(cell) the volume of the unit cell. When compared to the packing coeffficients of the two polymorphs of TM and the three polymorphs of TE[11], the results indicate that the packing of the co-crystals is in general more loose-fitting than that of the polymorphs with the TM-22bp co-crystal being the exception. Form III of TE is left out of consideration as the structure has voids and is thus very loosely packed.

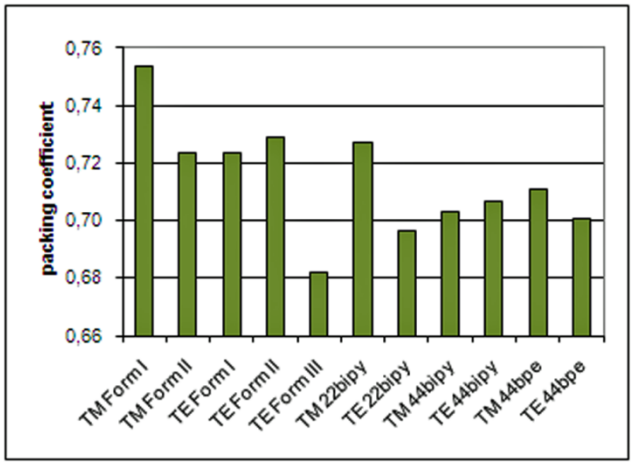

Fig. 5 Packing coefficients of the polymorphs of TM and TE and the bipyridine co-crystals

As the 2,2'-bipyridines are not hydrogen bonded to the TM/TE molecules in either of the co-crystal structures, the reason for the formation of structures is in the packing of the thiophanates and the template effect of the 22bp. The 22bp co-crystal with TM forms most likely because of the several simultaneous strong and weak hydrogen bonds between the TM molecules as well as favorable close packing. It is likely that the 22bp molecules template the formation of the rings of TM enabling this sort of clathrate packing to take place. There is some movement of the 22bp inside the ring and the MeCN molecule, which suggest that bigger guests could fit better in the ring cavity and in place of the MeCN. The packing coefficient of the 22bp co-crystal with TE, however, is the lowest of all the co-crystal stuctures, which suggest that favorable weak interactions must play a big role. As the amount of hydrogen bonding is the same as in the other structures, this structure is stabilized by the aromatic stacking interactions between the TE molecules.

The 4,4'-bipyridine and 1,2-bis(4-pyridyl)ethane co-crystals have low packing coefficients and are formed because of the strong hydrogen bonds between the 44bp/44bpe and thiophanate molecules. These strong hydrogen bonds are also the reason why the packing of the these co-crystals of TM and TE is more similar to each other than that of the 2,2'-bipyridine co-crystals. The 44bpe co-crystal with TM is the most densely packed of all the hydrogen bonded co-crystals, likely because of the formation of the two slightly different layers. Because of the efficient use of hydrogen bonds, the 44bpe co-crystal with TE has voids of 50 $Å^3$ and a lower packing coefficient than the other hydrogen bonded co-crystals.

Grinding

Having acquired such a group of similar co-crystals, we decided to use test whether the known co-crystals could be produced with liquid-assisted grinding. Compounds were weighed in the ratios of the known co-crystals and water:ethanol was used as solvent. The TM-22bp co-crystal is known to contain MeCN, but this was disregarded partly to see if a co-crystal that does not contain acetonitrile exists.

The TM-44bp and TE-22bp mixtures made the known co-crystals when grinded with water:ethanol, but the TE-44bp and TM-22bp mixtures did not (Fig. 6). The TE-44bp mixture PXRD

does not have peaks from pure 44bp or any of the known TE polymorphs. This could indicate another co-crystal that has better packing than the original co-crystal. The crystallization of such a co-crystal was attempted from ethanol without success. The TM-22bp PXRD is similar to the calculated pattern from the MeCN solvate of the co-crystal, indicating that the formation of the co-crystal may not depend on the presence of MeCN, and that there may be a co-crystal in which ethanol takes the place of MeCN. Attempts to crystallize this were also unsuccessful. New grinding experiments of TE-44bp and TM-22bp with 3 drops of 25% MeCN in H_2O were done to confirm the formation of the original co-crystals. Both the samples gave the pattern of the known co-crystal structure.

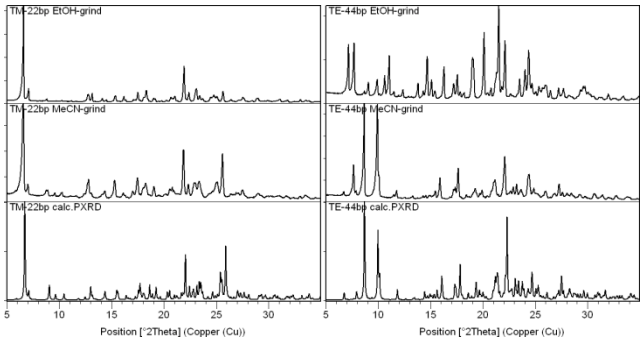

Fig. 6 PXRD patterns of the EtOH and MeCN grinding experiments of TM with 22bp (left) and TE with 44bp (right) compared to the patterns calculated from the structures.

Thermomicroscopy

Thermomicroscopy was used to investigate the melting behavior of the co-crystals. As both TM and TE decompose upon melting[10,11], we were unable to use melt film methods to produce the co-crystals. We wanted to know if the formation of a co-crystal could be determined with the thermomicroscope. The melting ranges for the co-crystals in Table 2 are very broad due to poor repeatability of the melting observations caused by interference from the unco-crystallized pure compounds and the changes in crystallite size when the co-crystals were produced with different methods.

The melting points of the TM-22bp co-crystal and both the TE co-crystals, however, do show a clear difference to the pure compounds, all melting at temperatures in between the melting points of the pure compounds, and the formation of these co-crystals can thus be recognized with thermomicroscopic observations. The TM-44bp co-crystal, however, melts only at the temperature where TM starts to decompose and can not be recognized in this manner from pure TM. If single crystals were not obtained to confirm the co-crystal formation, thermomicroscopy, which requires very little material, could still have been used together with powder diffraction to help verify at least three of the co-crystals.

The melting points of the found co-crystals are mostly lower than those of the pure actives, which is the opposite of what is generally preferred for agrochemical co-crystals. For TM and TE, making the melting point higher with co-crystals is unlikely because of the thermal decomposition of the actives upon melting. The co-crystals could still be viable forms for processing of formulations because of possible solubility differences and crystallite shape preferences.

Table 2 Approximate melting points (MP) of the compounds and co-crystals as determined by hot stage microscopy

Compound	MP (pure)	MP (22bp co-crystal)	MP (44bp co-crystal)
TM	167	110-120	160-170
TE	192	120-130	140-150
22bp	70	-	-
44bp	110	-	-

Conclusions

With the discovery of these six co-crystals, we have acquired further proof that TM and TE can include a number of guest molecules in their crystal lattices. The reasons for this behavior seem to be the large amount of hydrogen bond donors coupled to weak acceptors, the flexibility of the molecules, as well as the possibility for aromatic interactions. The two arms of the molecule being *ortho*-substituted in the benzene ring may also make the packing of the molecules somewhat difficult via forcing the sulfur and oxygen atoms quite close to each other unless guest molecules are included between the arms.

The N-H•••N-pyridine hydrogen bond was found to be a reliable synthon for co-crystal design with TM and TE. The inherent weakness of the N-H•••S=C hydrogen bond commonly used in the polymorphs and solvates of TM and TE is likely the cause, as was found for a more simple dithiooxamide by Piotrkowska *et al.*[27]

An important goal was to see how much the size difference of TM and TE affects the crystallization behavior and packing of the molecules. For the hydrogen bonded co-crystals of TM and TE the size difference of the molecules was found to effect the structures in a subtle manner. The main hydrogen bond pairing was always the same, but the size of the molecule influenced the usage of the rest of the donors and acceptors. In the TM co-crystals with 4,4'-bipyridine and 1,2-bis(4-pyridyl)ethane one N-H donor and all or most the C=S acceptors are unused, while in the TE co-crystal with 4,4'-bipyridine only a pyridine acceptor is unused and in the TE co-crystal with 1,2-bis(4-pyridyl)ethane all donors and acceptors are in use. This is because the larger molecules have more conformational freedom and can pack well even with more hydrogen bonds in use. For the 2,2'-bipyridine co-crystals the difference is not clear while TE makes a channel structure known to also fit other molecules and TM bouilds a clathrate type structure templated by the 2,2'-bipyridine.

The stoichiometric diversity in the co-crystals with the same bipyridines raises the question of whether there could be more co-crystals with different molar ratios like in the work of Trask *et al.*[28] on caffeine co-crystals. The TE-4,4'-bipyridine sample grinded with EtOH could be an example of this, but further investigation is required. We believe there are also numerous other possibilities for co-crystals as well as solvates of TM and TE. Similar molecules with flexible chains attached *ortho* on a benzene ring could also be reliable co-crystal formers and we plan on further investigating these.

Acknowledgements

We would like to thank the academy of Finland (proj. no. 116503) for partly funding the work and Dr. Heidi Saxell at BASF SE in Ludwigshafen, Germany for fruitful discussions.

Notes and references

University of Jyväskylä, Department of Chemistry, Nanoscience Center, P.O. Box 35, FI-40014 University of Jyväskylä, Finland. Fax: +358 14 260 4756; Tel: +358 14 260 4242; E-mail: maija.nissinen@jyu.fi

1 A. D. Bond, *CrystEngComm,* 2007, **9**, 833-834 (DOI: 10.1039/b708112j).
2 C. B. Aakeröy and D. J. Salmon, *CrystEngComm,* 2005, **7**, 439-448 (DOI:10.1039/b505883j).
3 O. Almarsson and M. J. Zaworotko, *Chem. Commun.,* 2004, **17**, 1889-1896 (DOI:10.1039/b402150a).
4 N. Blagden, M. de Matas, P. T. Gavan and P. York, *Adv. Drug Delivery Rev.,* 2007, **59**, 617-630 (DOI: 10.1016/j.addr.2007.05.011).
5 D. McNamara, S. Childs, J. Giordano, A. Iarriccio, J. Cassidy, M. Shet, R. Mannion, E. O'Donnell and A. Park, *Pharm. Res.,* 2006, **23**, 1888-1897 (DOI: 10.1007/s11095-006-9032-3).
6 *C07D 405/06 A01N 43/653. Pat.,* WO 2008/117037 A1, 02.10.2008.
7 *C07D 239/42 A01N 43/54. Pat.,* WO 2008/117060 A2, 02.10.2008.
8 G. R. Desiraju, *Angew. Chem. Int. Ed.,* 2007, **46**, 8342-8356 (DOI:10.1002/anie.200700534).
9 G. R. Desiraju, *Angew. Chem. Int. Ed Eng,* 1995, **34**, 2311-2327 (DOI:10.1002/anie.199523111).
10 E. Nauha, H. Saxell, M. Nissinen, E. Kolehmainen, A. Schäfer and R. Schlecker, *CrystEngComm,* 2009, **11**, 2536-2547 (DOI:10.1039/b905511h).
11 E. Nauha, A. Ojala, H. Saxell and M. Nissinen, *CrystEngComm,* 2011. (DOI:10.1039/C1CE05077J)
12 I. D. H. Oswald, W. D. S. Motherwell and S. Parsonsa, *Acta Cryst., Sect.B: Struct.Sci.,* 2005, **61**, 46-57 (DOI:10.1107/S0108768104028605).
13 H. W. Roesky and M. Andruh, *Coord. Chem. Rev.,* 2003, **236**, 91-119 (DOI: 10.1016/S0010-8545(02)00218-7).
14 I. D. H. Oswald, D. R. Allan, P. A. McGregor, W. D. S. Motherwell, S. Parsons and C. R. Pulham, *Acta Cryst., Sect.B: Struct.Sci.,* 2002, **58**, 1057-1066 (DOI:10.1107/S0108768102015987).
15 A. Ranganathan, V. R. Pedireddi, G. Sanjayan, K. N. Ganesh and C. N. R. Rao, *J. Mol. Struct.,* 2000, **522**, 87-94 (DOI: 10.1016/S0022-2860(99)00356-7).
16 S. Varughese and V. R. Pedireddi, *Chem. Eur. J.,* 2006, **12**, 1597-1609 (DOI:10.1002/chem.200500570).
17 T.-F. Tan, J. Han, M.-L. Pang, H.-B. Song, Y.-X. Ma and J.-B. Meng, *Cryst. Growth Des.,* 2006, **6**, 1186-1193 (DOI:10.1021/cg060009y).
18 B. Ye, M. Tong and X. Chen, *Coord. Chem. Rev.,* 2005, **249**, 545-565 (DOI: 10.1016/j.ccr.2004.07.006).
19 PANalytical B.V., 2006, **2.2b**.
20 G. M. Sheldrick, *Acta Cryst. A.,* 2008, **64**, 112-122 (DOI:10.1107/S0108767307043930).
21 Z. Otwinowski, D. Borek, W. Majewski and W. Minor, *Acta Cryst. A.,* 2003, **59**, 228-234 (DOI:10.1107/S0108767303005488).
22 C. F. Macrae, P. R. Edgington, P. McCabe, E. Pidcock, G. P. Shields, R. Taylor, M. Towler and J. van de Streek, *J. Appl. Cryst.,* 2006, **39**, 453-457 , (DOI: 10.1107/S002188980600731X).
23 R. K. Harris, *Analyst*, 2006, **131**, 351-373 (DOI: 10.1039/b516057j).
24 M. C. Etter and J. C. MacDonald, *Acta Cryst., Sect.B: Struct.Sci.*, 1990, **B46**; 256-262; J. Bernstein, R. E. Davis, L. Shimoni and N-L. Chung, *Angew. Chem. Int. Ed. Engl.*, 1995, **34**, 1555-1573.
25 A. I. Kitaĭgorodskiĭ, *Organic chemical crystallography*, Consultants Bureau, New York, 1961.
26 Calculation of Molecular Properties and Drug-likeness, Molinspiration, http://molinspiration.com/.
27 B. Piotrkowska, A. Wasilewska, M. Gdaniec and T. Polonski, *CrystEngComm*, 2008, **10**, 1421-1428 (DOI: 10.1039/b806061d).
28 A. V. Trask, J. van de Streek, W. D. S. Motherwell and W. Jones, *Cryst. Growth Des.,* 2005, **5**, 2233-2241 (DOI:10.1021/cg0501682)